Available online at www.sciencedirect.com
SCIENCE DIRECT
Biochimica et Biophysica Acta 1722 (2005) 175–182
BIOCHIMICA ET BIOPHYSICA ACTA
BBA
http://www.elsevier.com/locate/bba

Regular paper

Identification and characterization of a L-tyrosine decarboxylase in *Methanocaldococcus jannaschii*

Nicole D. Kezmarsky, Huimin Xu, David E. Graham[1], Robert H. White*

Department of Biochemistry, Virginia Polytechnic Institute and State University, Blacksburg, Virginia 24061-0308, USA

Received 9 September 2004; received in revised form 30 November 2004; accepted 2 December 2004
Available online 22 January 2005

Abstract

Methanofuran is the first coenzyme in the methanogenic pathway used by the archaeon *Methanocaldococcus jannaschii*, as well as other methanogens, to reduce CO_2 to methane. The details of the pathway for the biosynthesis of methanofuran and the responsible genes have yet to be established. A clear structural element in all known methanofurans is tyramine, likely produced by the decarboxylation of L-tyrosine. We show here that the *mfnA* gene at *M. jannaschii* locus MJ0050 encodes a thermostable pyridoxal phosphate-dependent L-tyrosine decarboxylase that specifically produces tyramine. Homologs of this gene are widely distributed among euryarchaea but are not specifically related to known bacterial or plant tyrosine decarboxylases.

Keywords: L-*Tyrosine decarboxylase; Coenzyme biosynthesis; Methanofuran; Methanocaldococcus jannaschii*

1. Introduction

Methanofuran [1] is the first coenzyme in the pathway used by methanogens to reduce CO_2 to methane [2]. The methyltrophic bacteria also appear to use methanofuran as a coenzyme in formaldehyde oxidation [3,4]. In the first step of CO_2 reduction in methanogenesis, the benzylic amino group of methanofuran reacts with CO_2 to form a carbamate, which is then reduced to *N*-formylmethanofuran [5]. The formate of the resulting *N*-formylmethanofuran is then transferred to tetrahydromethanopterin and subsequently reduced to methane [6]. Of all the methanogenic coenzymes, the biosynthesis of methanofuran has received the least attention [7,8]. Although methanogens produce various forms of methanofuran that differ in their side chains, all contain a conserved core structure with tyramine as a dominant element [9]. We proposed that this tyramine moiety is produced by the decarboxylation of L-tyrosine (Fig. 1) [7]. A search of the available genome sequences of methanogens failed to identify any gene annotated as a tyrosine decarboxylase but did identify a gene encoding a putative glutamate decarboxylase in *Methanocaldococcus jannaschii* (locus MJ0050). Considering that the known glutamate decarboxylases [10] and L-tyrosine decarboxylases are all members of same group II of pyridoxal 5′-phosphate (PLP)-dependent decarboxylases [11] and that there is no apparent reason for methanogens to produce a glutamate decarboxylase, we considered that the *M. jannaschii* enzyme could catalyze the decarboxylation of L-tyrosine, producing tyramine for methanofuran biosynthesis.

To establish the functional role of the MJ0050 gene, its protein product was heterologously expressed, purified and tested for decarboxylase activity against a wide range of amino acids. Unlike aromatic decarboxylases that catalyze the decarboxylation of many analogous amino acids [12] this enzyme is quite specific for L-tyrosine, which is consistent with its proposed role of supplying tyramine for methanofuran biosynthesis. As the first protein proposed to function specifically in methanofuran

* Corresponding author. Tel.: +1 540 231 6605; fax: +1 540 231 9070.
E-mail address: rhwhite@vt.edu (R.H. White).
[1] Current address: Department of Chemistry and Biochemistry and The Institute for Cellular and Molecular Biology, The University of Texas at Austin, 1 University Station A5300, Austin, TX 78712-0165, USA.

0304-4165/$ - see front matter © 2004 Elsevier B.V. All rights reserved.
doi:10.1016/j.bbagen.2004.12.003

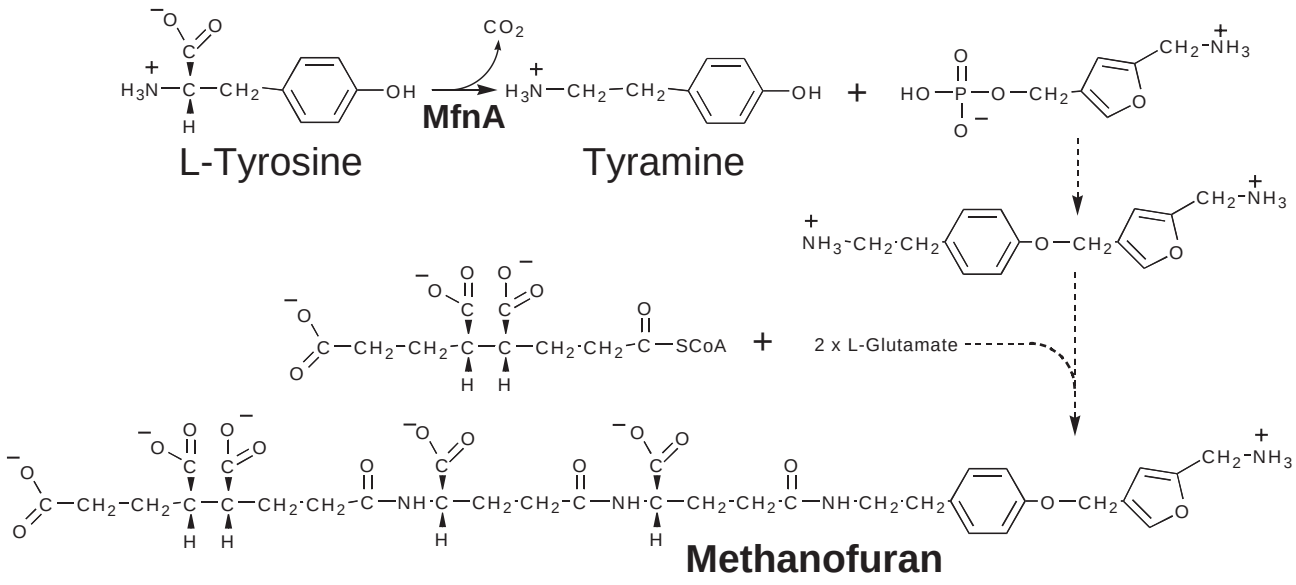

Fig. 1. Proposed biosynthetic pathway for methanofuran from tyrosine, a 2,4-disubstituted furan, two glutamates and a variable thioacyl chain such as 1, 3, 4, 6-hexanetetracarboxylic acid [7,8]. The MfnA protein catalyzes L-tyrosine decarboxylation to form tyramine.

biosynthesis, this enzyme is designated the MfnA enzyme and the respective gene, *mfnA*.

2. Materials and methods

2.1. Chemicals

The amino acids L-alanine, L-aspartic acid, 3,4-dihydroxy-L-phenylalanine, L-glutamic acid, L-homotyrosine, L-4-hydroxyphenylglycine, L-lysine, L-ornithine, *O*-phospho-L-threonine, L-phenylalanine, L-phenylglycine, L-serine, L-threonine, L-tryptophan, L-*m*-tyrosine, L-*p*-tyrosine (L-tyrosine) and D-tyrosine; the amines tryptamine, hydroxylamine and *O*-methylhydroxylamine; and the pH buffers 2-(*N*-cyclohexylamino)ethanesulfonic acid (CHES) and 2-[(2-hydroxy-1-1-bis[hydroxymethyl]ethyl)amino]ethanesulfonic acid (TES) were obtained from Sigma Chemical Co. Tyramine and L-homotyrosine were obtained from Fluka Chemical Co.

2.2. Cloning and expression of the M. jannaschii mfnA (MJ0050) gene

The *M. jannaschii mfnA* gene at locus MJ0500 (Swiss-Prot accession number Q60358) was amplified by PCR from genomic DNA using oligonucleotide primers synthesized by Invitrogen: Fwd (5′-GGTGGTCATATGAGAAACATG-CAGG -3′) and Rev (5′-GATCGGATCCTTAATCCCTTT-TAATAC -3′). PCR was performed as described previously [13,14] using a 50 °C annealing temperature. The primers introduced *Nde*I and a *Bam*HI sites at the 5′ and 3′ ends, respectively. The amplified PCR product was cloned by standard methods to make the recombinant plasmid pMJ0050 using the pT7-7 plasmid vector [14]. DNA sequences were verified by dye-terminator sequencing at the University of Iowa DNA facility. Plasmid pMJ0050 was transformed into *Escherichia coli* BL21-CodonPlus (DE3)-RIL (Stratagene) cells for protein expression. The transformed cells were grown in Luria-Bertani medium (200 ml; Difco) supplemented with 100 μg/ml ampicillin at 37 °C with shaking until they reached an absorbance at 600 nm of 1.0. Heterologous protein production was induced by the addition of lactose to a final concentration of 28 mM. After an additional culture of 2 h, the cells were harvested by centrifugation (5 min, 4000×*g*) and frozen at −20 °C.

2.3. Analysis of protein expression and protein purification

E. coli cells transformed with the pMJ0050 plasmid expressed the heterologous protein. The induction of the desired protein was confirmed by SDS-polyacrylamide gel electrophoresis (SDS-PAGE) analysis of total cellular proteins and showed that >60% of the cellular protein was the heterologous MfnA protein. The apparent mass of the expressed, denatured protein was determined by comparing protein migration to the migration of low molecular weight protein standards (Bio-Rad) separated by SDS-PAGE. Soluble cell-free extracts containing this protein were prepared by sonication and centrifugation as described previously [14]. MfnA protein was purified by heating, anion-exchange chromatography and gel-filtration chromatography [15]. The presence of the protein was clearly visible in each step of the purification by its intense yellow color. Analytical size-exclusion chromatography was performed at room temperature on a Superose 12HR column (1×30 cm; Amersham Biosciences) [15].

2.4. Identification of reaction products and analysis of enzymatic activity

Two different analytical methods (HPLC and gas chromatography–mass spectrometry (GC–MS)) were used to identify the products of the MfnA catalyzed reactions and to measure the ratio of product to substrate in the reaction after a specific incubation time. Specific activities of the MfnA enzyme were calculated from product:substrate ratios based on the known concentrations of L-tyrosine substrate and enzyme added to the standard assay. In a standard assay 5 μl of a 5 mM substrate solution was added to 50 μl of 50 mM TES/NaOH buffer (pH 7.15) containing 30 μg of MfnA. After incubation at 70 °C for 15 min the reaction was terminated by the addition of 100 μL methanol and the protein removed by centrifugation (5 min, 14,000×*g*). The remaining soluble substrates and products were measured either by HPLC or GC–MS. As can be seen in Fig. 2 the ratio of tyramine to tyrosine was linear over the 15 min time course of the fixed time assay. Known compounds were used to confirm retention times and mass spectral data. For HPLC analysis of aromatic compounds the methanol soluble substrates and products from the reaction mixture were diluted with 1 ml of 25 mM sodium acetate buffer (pH 6.0, 0.02% NaN_3) and 20 μl portions were separated and quantified using a Shimadzu SCL-6B HPLC with a C-18 reversed-phase column (AXXI Chrom octyldecyl silane column, 5 μm, 4.6 mm×25 cm). Isocratic elution was used with a solution of methanol (20 or 40% v/v) in 25 mM sodium acetate buffer (pH 6.0, 0.02% NaN_3) at a flow rate of 0.5 ml/min. The eluent was monitored by absorbance at 274 nm for L-4-hydroxyphenylglycine, 3,4-dihydroxyphenylalanine, L-homotyrosine, L-phenylalanine, L-phenylglycine, L-tyrosine, D-tyrosine, *m*-L-tyrosine, tyramine, tryptophan and tryptamine. Using these chromatographic conditions the substrates and products showed the following retention times in 20% methanol: 4-hydroxyphenylglycine, 5.4 min; 3, 4-dihydroxyphenylalanine, 6 min; L-tyrosine, 6.5 min; D-tyrosine, 6.5 min; *m*-L-tyrosine, 8 min; tyramine, 10.5 min. Using 40% methanol, tryptophan and tryptamine eluted respectively at 8 and 17 min. For GC–MS analyses of the amino acids and amine products, the reaction mixtures were evaporated to dryness, converted to the methyl ester trifluoroacetyl and/or trifluoroacetyl derivatives and analyzed by GC–MS as previously described [16]. Fig. 3 shows a typical GC–MS separation of the derivatives of tyramine and tyrosine that is representative of the separations observed. In each case base line separation of reaction substrate and products was observed and the area of the integrated signals was used to calculate the ratio of substrate to products. Fig. 3 also shows the mass spectra of the two peaks.

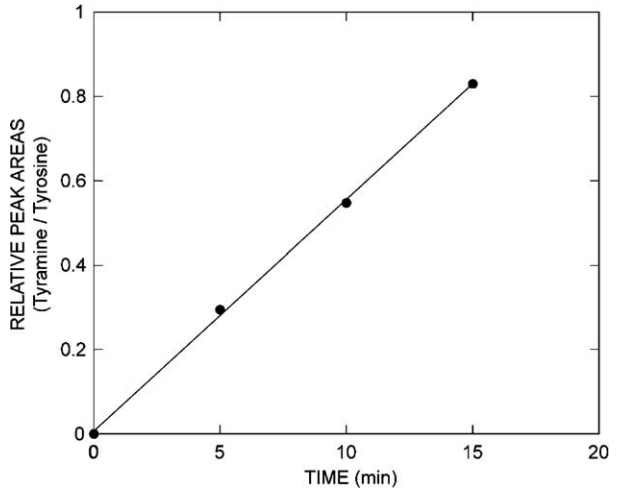

Fig. 2. In a standard tyrosine decarboxylase assay the MfnA protein catalyzes the production of tyramine from tyrosine with a linear ratio of product to substrate. The tyramine reaction product was separated from tyrosine by HPLC and quantified as described in the Materials and methods section.

2.5. Heat stability and pH optimum of the enzyme

To test the heat stability of the enzyme, purified MfnA in the standard assay buffer (50 μl of a 1 mg/ml solution) was incubated for 10 min at temperatures from 70 to 121 °C. Samples were heated in sealed tubes at temperatures from 70 to 110 °C and the temperature of 121 °C was obtained by autoclaving the sample. The resulting protein solutions were assayed for L-tyrosine decarboxylase activity using the standard assay at 70 °C. The effect of pH on L-tyrosine decarboxylase was studied using TES/NaOH (pH 6–8) or CHES/NaOH (pH 9–10) buffers.

2.6. Substrate specificity and enzyme inhibitors

The following amino acids were tested for their ability to serve as substrates for the L-tyrosine decarboxylase: L-alanine, L-aspartic acid, L-glutamic acid, L-homotyrosine, L-4-hydroxyphenylglycine, L-phenylalanine, L-phenylglycine, L-tryptophan, D-tyrosine, L-*m*-tyrosine and L-*p*-tyrosine (L-tyrosine). Hydroxylamine and *O*-methylhydroxylamine were tested as enzyme inhibitors by addition to the standard assay at a concentration of 2 mM.

2.7. Sequence alignment and phylogenetic analysis of mfnA homologs

The *M. jannaschii* MfnA protein sequence was used to query the non-redundant protein database at the National Center for Biotechnology Information using the BLASTP program (Version 2.2.6) [17] with the BLOSUM62 matrix and default gap costs for existence-11 and extension-1. Additional homologs were identified using similar methods to search partial genome sequences. Amino acid sequences from 47 homologs were aligned using the ClustalW program (Version 1.83) [18]; 363 amino acid positions that were deemed to be confidently aligned were selected for phylogenetic analysis. These protein sequences and their database accession numbers were from *Aeropyrum pernix* (SPL, gi|5105968; gi|14600392), *Arabidopsis thaliana*

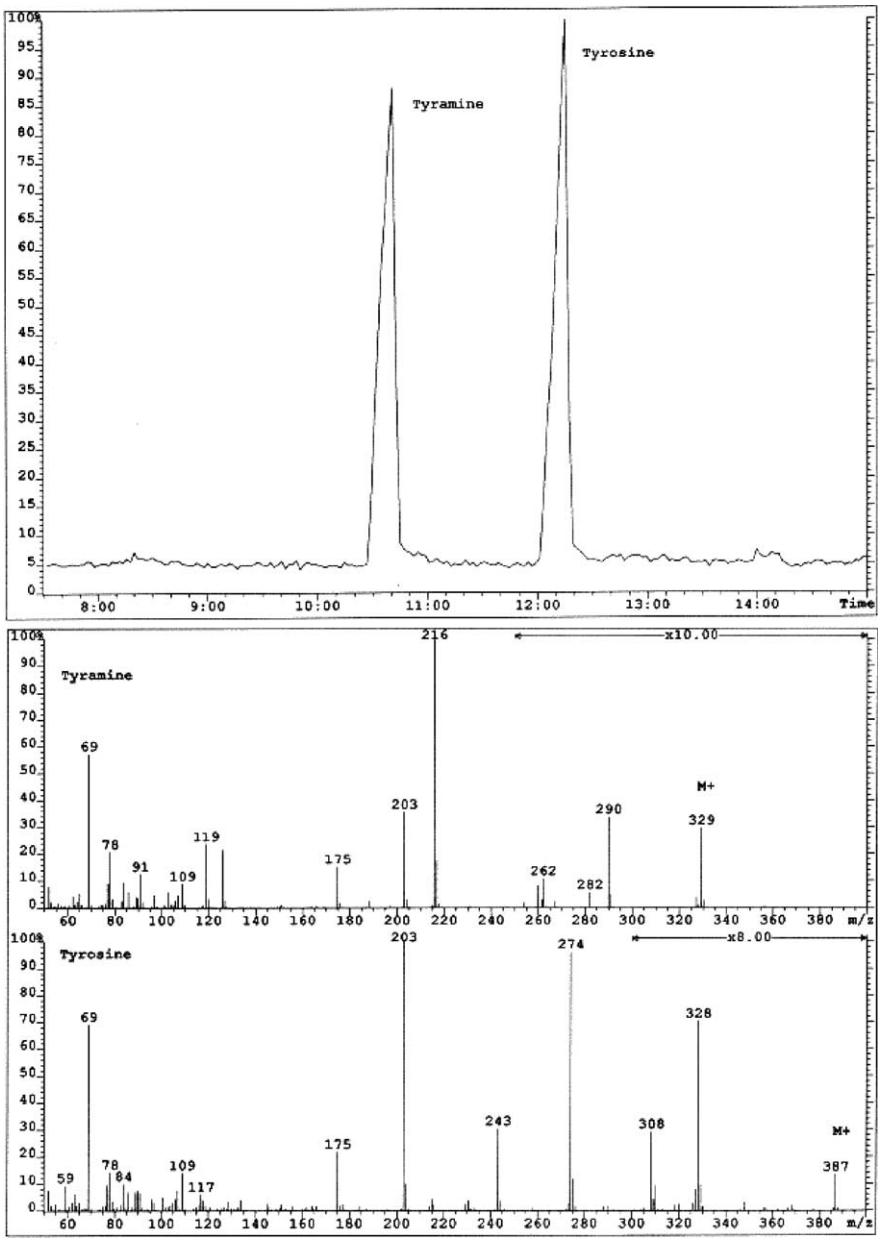

Fig. 3. GC–MS separation and mass spectra of the ditrifluoroacetyl derivatives of tyramine and the ditrifluoroacetyl methyl ester derivative of tyrosine. Tyrosine and tyramine were also resolved by HPLC separation, described in the Materials and methods section.

(GAD1, sp|Q42521; gi|15218445), *Archaeoglobus fulgidus* (TDC, gi|11499586; gi|11498921; gi|11499876; SPL, gi|4160532), *Caenorhabditis elegans* (DDC, sp|P34751; SPL, gi|1226312), *Catharanthus roseus* (DDC, sp|P17770), *Chloroflexus aurantiacus* (SPL, gi|22974905), *Ciona intestinalis* (SPL, gi|26554663), *Dictyostelium discoideum* (SPL,gi|30908928), *Drosophila melanogaster* (HDC, sp|Q05733; DDC, sp|P05031; GAD, sp|P20228; SPL, gi|21355963), *Enterobacter aerogenes* (HDC, sp|P28577), *Enterococcus faecium* (TDC, gi|22991708), *E. coli* (GadB, sp|P28302), *Felis silvestris catus* (GAD, sp|P14748), *Ferroplasma acidarmanus* (SPL, gi|22405553), *Gemmata obscuriglobus* (http://www.tigr.org), *Halobacterium* sp. (TDC, gi|15789600), *Homo sapiens* (HDC, sp|P19113; SPL, gi|10129683), *Lactococcus lactis* (GAD, sp|O30418), *Listeria monocytogenes* (GAD, sp|Q9EYW9), *Lycopersicon esculentum* (GAD, sp|P54767), *Methanocaldoccus jannaschii* (TDC, sp|Q60358), *Methanococcoides burtonii* (TDC, http://www.jgi.doe.gov), *Methanococcus maripaludis* (TDC, gi|45357694), *Methanogenium frigidum* (TDC, http://psychro.bioinformatics.unsw.edu.au), *Methanopyrus kandleri* (TDC, gi|20094936), *Methanosarcina acetivorans* (TDC, gi|20088905), *Methanothermobacter thermautotrophicus* (TDC, gi|15679127), *Morganella morganii* (HDC, sp|P05034), *Neurospora crassa* (SPL, gi|32413134), *Petroselinum crispum* (TDC, sp|Q06086), *Petunia hybrida* (GAD, sp|Q07346), *Pyrococcus abyssi* (TDC, gi|14521418), *Pyrococcus furiosus*

(TDC,gi|18977531), *Saccharomyces cerevisiae* (GAD, sp|Q04792; SPL, gi|6320500), *Shewanella oneidensis* (gi|24347590) and *Sus scrofa* (DDC, sp|P80041).

The phylogeny of these homologs was inferred by the protein maximum likelihood criteria using the PROML program (Version 3.6a3) [19] with the Jones, Taylor and Thornton model of amino acid changes and a γ distribution of positional rates of change (coefficient of variation=0.64). Bootstrap proportions were calculated by using SEQBOOT, PROML and CONSENSE programs [19] to create and evaluate 100 resampled alignments. An alternative tree was identified by the protein distance method using the PROTDIST and NEIGHBOR programs (Version 3.6a3) [19], with the same parameters described for the PROML program.

3. Results

3.1. Purification of the MfnA protein

The final purified MfnA protein was yellow and showed absorbance maxima at 277, 335 nm and 419 nm (Fig. 4) expected for a PLP containing protein [20,21] and the same as observed in the aromatic amino acid decarboxylases [12]. The protein formed a single band when analyzed by SDS-PAGE with an apparent mass of 45 kDa, consistent with the predicted mass of 48 kDa based on nucleotide sequence. The MfnA protein eluted from the analytical gel filtration column with an apparent mass of 90 kDa, suggesting that the protein forms a homodimer.

3.2. Characteristics of the enzymatic reaction

The enzyme was tested using the standard assay with L-tyrosine, *m*-L-tyrosine, L-4-hydroxyphenylglycine, L-phe-

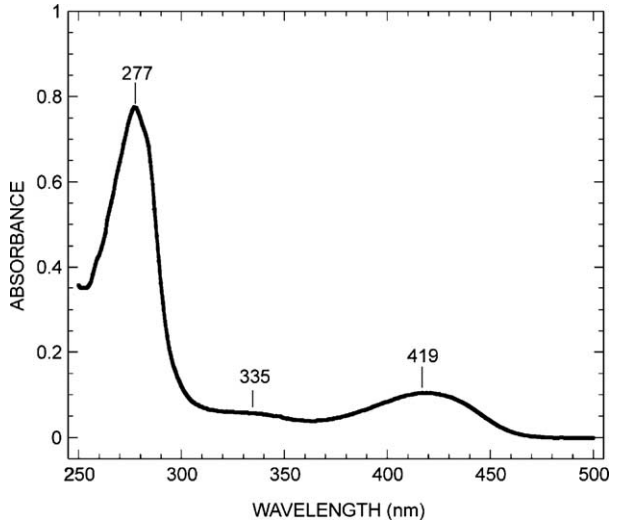

Fig. 4. Purified L-tyrosine decarboxylase from *M. jannaschii* (0.81 mg/ml) has a UV-visible spectrum characteristic of PLP-dependent proteins. Absorbance maxima are indicated above the absorbance curve.

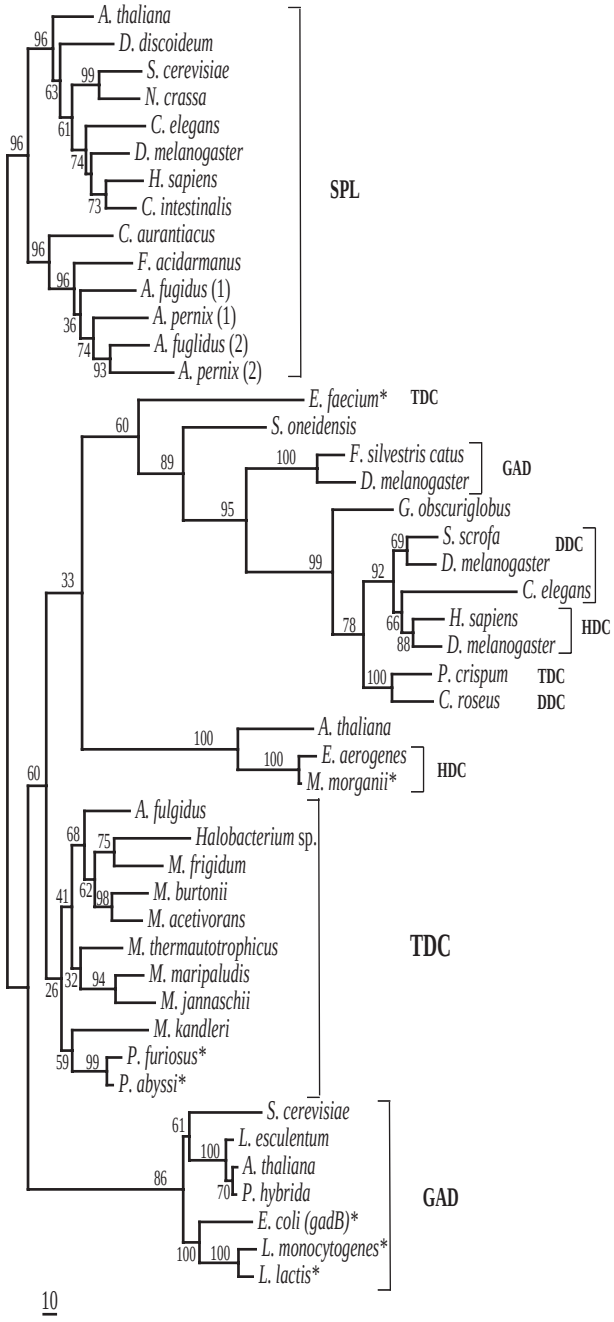

Fig. 5. Phylogeny of MfnA and homologous members of the PLP-dependent transferase superfamily [22] inferred by the protein maximum likelihood criteria. Sequences are bracketed by presumed function: sphinganine-1-phosphate lyase (SPL; EC 4.1.2.27), L-glutamate decarboxylase (GAD; EC 4.1.1.15), aromatic L-amino acid (DOPA) decarboxylase (DDC; EC 4.1.1.28), histidine decarboxylase (HDC; EC 4.1.1.22) and L-tyrosine decarboxylase (TDC; EC 4.1.1.25). Paralogs of the *A. fulgidus* and *A. pernix* genes are distinguished by numbers in parentheses following their species name. The tree was arbitrarily rooted using the SPL sequences as an outgroup. Bootstrap proportions are indicated for branches supported by a plurality of bootstrap replicates. Sequences marked with an asterisk are found adjacent to putative amino acid transporter genes in their respective genomes. An analysis using protein distance and neighbor joining methods produced an equivalent tree that differs only in its local placement of the *M. thermautotrophicus* TDC and *S. cerevisiae* GAD sequences. The scale bar indicates 10 predicted amino acid replacements per 100 positions.

nylglycine, L-phenylalanine, L-homotyrosine, L-aspartate, L-serine, L-threonine, L-phosphothreonine, L-glutamate, L-tryptophan, L-ornithine, L-alanine, L-lysine, and D-tyrosine as substrates. No amino acid except L-tyrosine, which was completely decarboxylated, was decarboxylated to an extent of greater than 1%. Incubation with a mixture of L-serine, L-threonine, L-phosphothreonine, L-glutamate and L-ornithine for 4 h with 0.5 mg of the heated cell-free extract containing MfnA showed 95% decarboxylation of aspartate and 80% decarboxylation of glutamate. No decarboxylation of the other amino acids was observed. The sole reaction product from L-tyrosine was found to be tyramine based on GC–MS analysis (Fig. 3) of the ditrifluoroacetyl derivative (M^+=329 m/z) and HPLC retention times compared to the known standards. The enzyme had a specific activity for the decarboxylation of L-tyrosine of 1.1±0.12 U mg^{-1} protein with a K_m of 1.6±0.29 mM (1 U=1 μmol tyrosine decarboxylated min^{-1}). The enzyme retained full activity after it was heated at a temperature of 100 °C for 10 min and retained 42% of its activity after 10 min at 110 °C. No activity was observed after 10 min at 121 °C. The enzyme was completely inhibited by the addition of 2 mM hydroxylamine and *O*-methylhydroxylamine to the assay mixture. The pH optimum of the enzyme was between pH 7.5 and 8.5.

3.3. Sequence analysis and evolution

Closely related homologs of *mfnA* are found in all complete methanoarchaeal genome sequences, as well as in

Fig. 6. Alignment of the *M. jannaschii* MfnA sequence with homologous class II PLP-dependent amino acid decarboxylases. The tyrosine decarboxylase (TDC) sequence from *M. jannaschii* is similar to those of orthologous *M. thermautotrophicus* and *P. furiosus* proteins, but is distantly related to the sequences of histidine decarboxylases (HDC) from *M. morganii* and human, tyrosine decarboxylases from *E. faecalis* and parsley, pig dopamine decarboxylase (DDC), or *E. coli* glutamate decarboxylase (GAD). The conserved PLP-binding lysine residue (Lys245) is indicated with an asterisk. Positions of identically conserved residues are shown in white on black and regions of similarly conserved residues are boxed.

A. fulgidus, *Halobacterium* sp. and *Pyrococcus* spp. (Fig. 5). This phylogenetic pattern suggests that the genes are orthologs and were vertically inherited in the euryarchaeal lineage. These L-tyrosine decarboxylase proteins are members of the aromatic amino acid (DOPA) decarboxylase structural family of proteins, which belongs to the PLP-dependent transferase superfamily [22]. This superfamily includes all of the group II decarboxylases of histidine (HDC), L-tyrosine (TDC), glutamate (GAD) and various aromatic amino acids (DDC), as well as the sphinganine phosphate lyase (SPL) (Fig. 5). As observed for the other amino acid decarboxylases, the L-tyrosine decarboxylases do not cluster in a single group [11]. The archaeal L-tyrosine decarboxylases are not specifically related to the previously identified L-tyrosine decarboxylases from bacteria (*Enterococcus faecalis* [23] and *Lactobacillus brevis* [24]) or eukaryotes (parsley [25]).

All group II decarboxylase proteins form homodimers and share a conserved lysine residue that binds the PLP cofactor (Lys245 in *M. jannaschii* MfnA, Fig. 6) as well as a set of active site residues that promote decarboxylation (His132, Thr181 and Asp206) [26,27]. Residues that interact with the substrate amino acid side chain are poorly conserved between TDC and DDC proteins. Because several of the residues that confer amino acid substrate specificity are provided by the adjacent subunit they are more difficult to identify by primary sequence analysis [26]. A flexible loop is believed to exclude the solvent from the active site of DDC during catalysis [12]; this region is also poorly conserved in TDC sequences.

4. Discussion

Glutamate decarboxylase has been isolated from a wide range of biological materials from bacteria to brains [28], where it catalyzes the formation of 4-aminobutyrate from L-glutamate. The family of group II PLP-dependent amino acid decarboxylases, which includes previously characterized glutamate and tyrosine decarboxylases has a sole representative in the genome of *M. jannaschii*. This MJ0050 gene was previously annotated as a L-glutamate decarboxylase. However, the requirement for such a reaction in the metabolism of the methanogenic archaea is far from clear. To test the specificity of this enzyme we have purified the heterologously expressed enzyme and demonstrated that it specifically catalyzes L-tyrosine decarboxylation. These results combined with the presence of orthologous genes in genomes of all methanofuran-producing archaea identify this first gene in methanofuran biosynthesis, which should be designated *mfnA*.

Catabolic tyrosine decarboxylases have been purified and cloned from the bacteria *E. faecalis* [23,29] and *L. brevis* [30]. These enzymes, which share 75% amino acid sequence identity, both form catalytically active homodimers [29,30], function optimally near pH 5.0 and have similar kinetic properties. Purified *E. faecalis* enzyme has a specific activity of 115 U mg^{-1} protein [29] and a K_m for L-tyrosine of 0.36 mM [31]. Similarly the *L. brevis* enzyme has a specific activity of 998 U mg^{-1} protein and a K_m of 0.63 mM [30]. Like many of the bacterial homologs shown in Fig. 5, these tyrosine decarboxylase genes in *E. faecalis* and *L. brevis* are genetically linked to putative tyrosine/tyramine antiporters. The combined system consumes protons and raises the cells' local pH.

In contrast to these highly active catabolic tyrosine decarboxylases, anabolic tyrosine decarboxylases have lower catalytic activities. The L-tyrosine/L-DOPA decarboxylase from the plant *Thalictrum rugosum* functions in isoquinoline alkaloid biosynthesis. Compared to the *E. faecalis* and *L. brevis* enzymes the plant enzyme has a lower K_m for tyrosine (0.27 mM), a lower specific activity (0.18 U mg^{-1} protein) and a higher pH optimum (8.4) for activity [32,33]. The anabolic MfnA protein described here has a comparable K_m for tyrosine (1.6 mM), a low specific activity for tyrosine decarboxylation and functions optimally near neutral pH.

Although the *M. jannaschii* MfnA protein catalyzes the same reaction and belongs to the same group II family of PLP-dependent enzymes as the bacterial and plant tyrosine decarboxylases, it shares less than 25% amino acid identity with those homologs. The archaeal *mfnA* homologs share a single common ancestor, suggesting that the gene evolved early in the euryarchaeal lineage. In contrast, bacteria have frequently recruited members of this group II decarboxylase family for new functions.

Acknowledgements

This work was supported by U. S. National Science Foundation Grant MCB 0231319 to R. H. W. We thank Kim Harich for assistance with the GC–MS analyses.

References

[1] J.A. Leigh, K.L. Rinehart Jr., R.S. Wolfe, Methanofuran (carbon dioxide reduction factor), a formyl carrier in methane production from carbon dioxide in *Methanobacterium*, Biochemistry 24 (1985) 995–999.

[2] A.A. DiMarco, T.A. Bobik, R.S. Wolfe, Unusual coenzymes of methanogenesis, Annu. Rev. Biochem. 59 (1990) 355–394.

[3] L. Chistoserdova, J.A. Vorholt, R.K. Thauer, M.E. Lidstrom, C1 transfer enzymes and coenzymes linking methylotrophic bacteria and methanogenic Archaea, Science 281 (1998) 99–102.

[4] B.K. Pomper, J.A. Vorholt, Characterization of the formyltransferase from *Methylobacterium extorquens* AM1, Eur. J. Biochem. 268 (2001) 4769–4775.

[5] S. Bartoschek, J.A. Vorholt, R.K. Thauer, B.H. Geierstanger, C. Griesinger, *N*-carboxymethanofuran (carbamate) formation from methanofuran and CO_2 in methanogenic archaea. Thermodynamics and kinetics of the spontaneous reaction, Eur. J. Biochem. 267 (2000) 3130–3138.

[6] T.A. Bobik, A.A. DiMarco, R.S. Wolfe, Formyl-methanofuran synthesis in *Methanobacterium thermoautotrophicum*, FEMS Microbiol. Rev. 7 (1990) 323–326.
[7] R.H. White, Biosynthesis of the 2-(aminomethyl)-4-(hydroxymethyl)-furan subunit of methanofuran, Biochemistry 27 (1988) 4415–4420.
[8] D.E. Graham, R.H. White, Elucidation of methanogenic coenzyme biosynthesis: from spectroscopy to genomics, Nat. Prod. Rep. 19 (2002) 133–147.
[9] R.H. White, Structural diversity among methanofurans from different methanogenic bacteria, J. Bacteriol. 170 (1988) 4594–4597.
[10] B. Maras, G. Sweeney, D. Barra, F. Bossa, R.A. John, The amino acid sequence of glutamate decarboxylase from *Escherichia coli*. Evolutionary relationship between mammalian and bacterial enzymes, Eur. J. Biochem. 204 (1992) 93–98.
[11] E. Sandmeier, T.I. Hale, P. Christen, Multiple evolutionary origin of pyridoxal-5′-phosphate-dependent amino acid decarboxylases, Eur. J. Biochem. 221 (1994) 997–1002.
[12] S. Ishii, H. Hayashi, A. Okamoto, H. Kagamiyama, Aromatic L-amino acid decarboxylase: conformational change in the flexible region around Arg334 is required during the transaldimination process, Protein Sci. 7 (1998) 1802–1810.
[13] M. Graupner, H. Xu, R.H. White, Identification of an archaeal 2-hydroxy acid dehydrogenase catalyzing reactions involved in coenzyme biosynthesis in methanoarchaea, J. Bacteriol. 182 (2000) 3688–3692.
[14] M. Graupner, H. Xu, R.H. White, Identification of the gene encoding sulfopyruvate decarboxylase, an enzyme involved in biosynthesis of coenzyme M, J. Bacteriol. 182 (2000) 4862–4867.
[15] H. Li, H. Xu, D.E. Graham, R.H. White, The *Methanococcus jannaschii* dCTP deaminase is a bifunctional deaminase and diphosphatase, J. Biol. Chem. 278 (2003) 11100–11106.
[16] L. Zheng, R.H. White, V.L. Cash, D.R. Dean, Mechanism for the desulfurization of L-cysteine catalyzed by the nifS gene product, Biochemistry 33 (1994) 4714–4720.
[17] S.F. Altschul, T.L. Madden, A.A. Schaffer, J. Zhang, Z. Zhang, W. Miller, D.J. Lipman, Gapped BLAST and PSI-BLAST: a new generation of protein database search programs, Nucleic Acids Res. 25 (1997) 3389–3402.
[18] J.D. Thompson, D.G. Higgins, T.J. Gibson, CLUSTAL W: improving the sensitivity of progressive multiple sequence alignment through sequence weighting, position-specific gap penalties and weight matrix choice, Nucleic Acids Res. 22 (1994) 4673–4680.
[19] J. Felsenstein, PHYLIP (Phylogeny Inferenc Package), 3.6a2.1 ed., Department of Genetics, University of Washington, Seattle, 2001.
[20] P. Fasella, Pyridoxal phosphate, Annu. Rev. Biochem. (1967) 185–210.
[21] A.E. Braunstein, Amino group transfers, in: P.D. Boyer (Ed.), The Enzymes, vol. IX, Academic Press, New York, 1973, pp. 739–781.
[22] A.G. Murzin, Structural classification of proteins: new superfamilies, Curr. Opin. Struct. Biol. 6 (1996) 386–394.
[23] N. Connil, Y. Le Breton, X. Dousset, Y. Auffray, A. Rince, H. Prevost, Identification of the *Enterococcus faecalis* tyrosine decarboxylase operon involved in tyramine production, Appl. Environ. Microbiol. 68 (2002) 3537–3544.
[24] P. Lucas, J. Landete, M. Coton, E. Coton, A. Lonvaud-Funel, The tyrosine decarboxylase operon of *Lactobacillus brevis* IOEB 9809: characterization and conservation in tyramine-producing bacteria, FEMS Microbiol. Lett. 229 (2003) 65–71.
[25] P. Kawalleck, H. Keller, K. Hahlbrock, D. Scheel, I.E. Somssich, A pathogen-responsive gene of parsley encodes tyrosine decarboxylase, J. Biol. Chem. 268 (1993) 2189–2194.
[26] P. Burkhard, P. Dominici, C. Borri-Voltattorni, J.N. Jansonius, V.N. Malashkevich, Structural insight into Parkinson's disease treatment from drug-inhibited DOPA decarboxylase, Nat. Struct. Biol. 8 (2001) 963–967.
[27] C. Momany, R. Ghosh, M.L. Hackert, Structural motifs for pyridoxal-5′-phosphate binding in decarboxylases: an analysis based on the crystal structure of the *Lactobacillus* 30a ornithine decarboxylase, Protein Sci. 4 (1995) 849–854.
[28] E.A. Boeker, E.E. Snell, Amino acid decarboxylases, in: P.D. Boyer (Ed.), The Enzymes, vol. VI, Academic Press, New York, 1972, pp. 217–253.
[29] T. Borresen, N.K. Klausen, L.M. Larsen, H. Sorensen, Purification and characterisation of tyrosine decarboxylase and aromatic-L-amino-acid decarboxylase, Biochim. Biophys. Acta 993 (1989) 108–115.
[30] V. Moreno-Arribas, A. Lonvaud-Funel, Purification and characterization of tyrosine decarboxylase of *Lactobacillus brevis* IOEB 9809 isolated from wine, FEMS Microbiol. Lett. 195 (2001) 103–107.
[31] A.P. Phan, T.T. Ngo, H.M. Lenhoff, Tyrosine decarboxylase. Spectrophotometric assay and application in determining pyridoxal-5′-phosphate, Appl. Biochem. Biotechnol. 8 (1983) 127–133.
[32] I. Marques, P.E. Brodelius, Elicitor-induced L-tyrosine decarboxylase from plant-cell suspension-cultures: 1. Induction and purification, Plant Physiol. 88 (1988) 46–51.
[33] I. Marques, P.E. Brodelius, Elicitor-induced L-tyrosine decarboxylase from plant-cell suspension-cultures: 2. Partial characterization, Plant Physiol. 88 (1988) 52–55.